Kerr Effect and Wide Angle Light-Scattering Studies of a Para-Aromatic Polyamide in Dilute Solution

A. J. Shere,* M. Sethumadhavan, and R. S. Stein

University of Massachusetts, Amherst, Massachusetts 01003

R. F. Saraf

IBM Watson Research Center, Yorktown, New York 10598

R. A. Gaudiana, P. Mehta, and T. Adams

Polaroid Corporation, Cambridge, Massachusetts 02139

Received November 30, 1995; Revised Manuscript Received December 22, 1995[⊗]

ABSTRACT: The geometric and optical properties of a para-aromatic polyamide are characterized using wide angle light scattering and electric birefringence. The polydispersity correction was applied theoretically by assuming the most probable distribution. The aromatic polyamide studied can be satisfactorily modeled as a Kratky−Porod wormlike chain with a presistence length of 220 ± 50 Å and an optical unit anisotropy ratio of 2.2 ± 0.3 in tetrahydrofuran. The refractive index of 1.67 ± 0.03 is comparable to that of similar polyamides. The high persistence length of the polymer chain and the high inherent optical anisotropy of the repeat unit are found to be responsible for the exceptionally high birefringence observed in the oriented films. It is also conclusively established that there is no aggregation in the absence of moisture.

Introduction

Over the last decade many processable, orientable polyamides have been synthesized,[1−3] but they cannot be utilized in most optical applications due to their visible absorption characteristics and crystallinity which causes scattering. The class of para-linked polyamides synthesized by Rogers et al.[4−7] are nonabsorbing in the visible wavelength range and soluble, e.g., several are soluble in THF and acetone, and may be processed into highly oriented, transparent ($X_c \sim 5\%$), highly birefringent films and fibers suitable for optical applications. Orienting these rodlike polymers (persistence length typically 200−300 Å[7]) via extrusion of their solutions is made more difficult by the absence of lyotropic behavior.

The goal of the present investigation is to attempt to determine the basis for the exceptionally high values of Δn observed in oriented films of these polyamides. To accomplish this, we have characterized the geometric and optical properties of the polyamide shown in Figure 1a. In particular we have studied the shape of the molecule by examining its optical polarizability anisotropy, $\alpha_{||} - \alpha_{\perp}$, where $\alpha_{||}$ and $\alpha_{\perp}$ are optical polarizabilities of the polymer chain, parallel and perpendicular to the end-to-end vector, respectively. Wide angle light-scattering measurements in THF were used to determine the weight-average molecular weight and the radius of gyration.

Electric birefringence has been used extensively in the characterization of optical properties of polymers and small molecules.[8−11] The optical anisotropy data obtained from Kerr measurements may be used in conjunction with wide angle light scattering to determine the rigidity of a polymer chain, i.e., Kuhn or persistence length.[12,13] Moreover, the Kerr effect is highly sensitive to the optical anisotropy and the geometric arrangement of Kuhn segments which makes it a particularly useful technique for the determination of molecular aggregation.[13−15] Hence, we have measured the Kerr constant of this polyamide along with the optical anisotropy ratio of a model compound (Figure 1b) of the repeat unit to probe both the rigidity and the state of aggregation of this polymer.

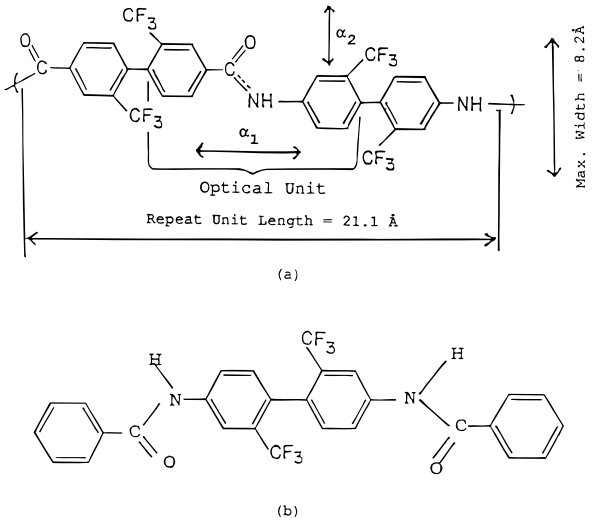

Figure 1. (a) Chemical repeat unit of the para-linked aromatic polyamide used for this study. α_1 and α_2 are the optical polarizabilities of the optical unit, parallel and perpendicular to the polymer backbone, respectively. (b) Chemical structure of the compound used to model the repeat unit of the polyamide studied.

Theory

Persistant Chain Model. The molecular chain anisotropy ratio, $\zeta^2 = (\alpha_{||} - \alpha_{\perp})^2/(\alpha_{||} + 2\alpha_{\perp})^2$, for a Porod−Kratky wormlike chain[16] is given by[17]

$$\zeta^2 = \frac{2}{27}\epsilon^2\frac{1}{x}\left(1 - \frac{1}{3x} + \frac{1}{3x}e^{-3x}\right) \qquad (1)$$

where $\epsilon = (\alpha_1 - \alpha_2)/\alpha_o$ and $x = L/a$. L is the contour length, and a is the persistence length of the polymer

[⊗] Abstract published in *Advance ACS Abstracts,* February 15, 1996.

0024-9297/96/2229-2088$12.00/0

chain. α_1 and α_2 are optical polarizabilities parallel and perpendicular to the optical unit as indicated in Figure 1a. $\alpha_1 - \alpha_2$ is the optical unit anisotropy, and $\alpha_o = (\alpha_1 + 2\alpha_2)/3$ is the mean optical polarizability of the optical unit. Figure 1a illustrates the chemical structure of the repeat unit of the para-linked aromatic polyamide used for this study. The optical unit is chosen to be the unit within which electrons are localized due to orthogonal orientation of phenyl rings of the biphenyl moieties. This choice assurrs the group additivity of the polarizability tensors of the optical units. According to this definition, a repeat unit consists of two optical units. The dimensions of the repeat unit are also shown in Figure 1a. Note that $\epsilon = 3$ for a rodlike optical unit with $\alpha_1 >>> \alpha_2$.

Kerr Effect. The Kerr law[18] states that the induced birefringence, Δn, at a given wavelength relates to the applied electric field strengths as

$$\Delta n = n_{||} - n_{\perp} = B\lambda E^2$$

where $n_{||}$ and $n_{\perp}$ are the refractive indices parallel and perpendicular to the electric field of strength E. This law is invalid for very high E. B is the Kerr constant of the medium which depends on the optical anisotropy of the chain, and λ is the wavelength of the light in the medium. The units of B and E are cm/statvolt^2 and statvolt/cm, respectively.

We have adopted the procedure outlined by LeFevre[9] for obtaining Kerr constant of a solute. Based on their formulation, the specific Kerr constant of a solute at infinite dilution is given as[19]

$$ {}_sK_2 = {}_sK_1(1 - a_2 + a_3 + a_4 - Ha_3 - Ja_1\epsilon_1) \quad (2)$$

The specific Kerr constant, ${}_sK_1$, of the solvent is given by ${}_sK_1 = 6n_1\lambda B_1/((n_1^2 + 2)^2(\epsilon_1 + 2)^2 d_1)$, where B_1 is the Kerr constant, n_1 is the refractive index, ϵ_1 is the dielectric constant, and d_1 is the density of the solvent. $H = 4n_1^2/(n_1^2 + 2)$, and $J = 2/(\epsilon_1 + 2)$. H, J, and ${}_sK_1$ are constants for a given solvent at a specified temperature. a_1, a_2, a_3, and a_4 are obtained by linear extrapolation of the dielectric constant, density, refractive index, and the Kerr constant of the solution to infinite dilution as $\epsilon = \epsilon_1 (1 + a_1 w_2)$, $d = d_1(1 + a_2 w_2)$, $n = n_1 (1 + a_3 w_2)$, and $B = B_1(1 + a_4 w_2)$, where w_2 is the weight fraction of the polymer in the solution.

For monodisperse polymer molecules, neglecting the permanent dipole moment contribution, the ratio of the square of optical polarizability anisotropy to the molecular weight is given by[20]

$$\frac{(\alpha_{||} - \alpha_{\perp})^2}{M} = \frac{405kT}{4\pi N_A}{}_sK_2 \quad (3)$$

where N_A is the Avogadro number, k is the Boltzmann constant, T is the absolute temperature, and M is the polymer molecular weight. Equation 3 is applicable in the present study since the dipole moment of the polyamide shown in Figure 1a is expected to be small based on the molecular structure. The components of the dipole moment along the polymer backbone due to the carbonyl groups and CF_3 groups cancel each other, and the component perpendicular to the backbone will add up to a negligible amount due to the random orientation of this component about the polymer backbone with each additional monomer unit. Our estimate based on the error analysis of Kerr effect measurement is that the permanent dipole moment of the polyamide studied is <5.0 D.

The polydispersity of the polyamide is taken into account by appropriately modifying the equation relating the optical anisotropy to the Kerr constant. Since the polyamide is synthesized by polycondensation, we assume the molecular weight distribution to be the most probable distribution,[21,22] $f(n) = y^2 n \exp(-yn)$, where $y = 2/n_w$, $f(n)$ is the weight fraction distribution, n is the degree of polymerization, and n_w is the weight-average degree of polymerization. The experiment determination of $f(n)$ be gel permeation chromatography is not possible due to the specific interaction of the polyamide with the column material. Since the experimentally obtained specific Kerr constant is the weight average of specific Kerr constants of the individual species, the weight-average ratio given in eq 4 is calculated by convoluting $(\alpha_{||} - \alpha_{\perp})^2/M$ for a wormlike chain from eq 1 with $f(n)$:

$$\left[\frac{(\alpha_{||} - \alpha_{\perp})^2}{M}\right]_{ave} = \frac{2\alpha_o{}^2\epsilon^2}{3M_o}\left[\frac{1}{\beta} - \frac{y}{3\beta^2} + \frac{y^2}{3\beta^2(y + 3\beta)}\right] \quad (4)$$

with $\beta = M_o/aM_L$. n_w is the weight-average degree of polymerization, M_o is the molecular weight of the optical unit, and M_L is the molecular weight per unit contour length of the polymer chain. Equation 4 has three unknowns: a, n_w, and ϵ. In order to estimate these parameters, we employ wide angle light scattering.

Light Scattering from Stiff Chains. Nagai[17] has calculated the structure factor for monodisperse wormlike polymer chains consisting of anisotropic scattering segments. The Rayleigh ratios, R_{Hv} and R_{Vv}, are given in terms of a, ϵ, and L. Following the polydispersity treatment due to Zimm,[23] we have evaluated the total scattering, $R(q) = R_{Hv} + R_{Vv}$, for polydisperse wormlike chains as

$$\frac{Kc}{R(q)} = \frac{1}{M_oA}\left[1 - \frac{B}{A}q^2 + O(q^4)\right] \quad (5)$$

where A and B are functions of y, β, and ϵ and are listed in the Appendix. The apparent molecular weight and radius of gyration are thus given by

$$M_{app} = M_oA \quad (6a)$$

$$R^2{}_{gapp} = -3\frac{B}{A} \quad (6b)$$

The above two equations and eq 4 for the Kerr effect are solved simultaneously to obtain the molecular parameters a, ϵ, and n_w.

Differential Refractometry. The Dale−Gladstone relation for differential refractive index increment in terms of polymer refractive index, n_2, and specific volume, V_2, is $dn/dc = V_2(n_2 - n_1)$, where n_1 is the solvent refractive index. The mean optical polarizability of the optical unit is calculated using the Lorentz−Lorenz equation, $(n_2^2 - 1)/(n_2^2 + 1) = (4\pi/3)N_p\alpha_o$, where N_p is the number density of submolecules with mean polarizability α_o.

Experimental Section

Kerr Effect. Electric birefringence was determined using the null technique for retardation measurement.[11] In this method two Kerr cells, one filled with the reference fluid and the other with the sample fluid, are placed in the optical path

between crossed polarizers. If the Kerr constants of the sample fluid and the reference fluid are of opposite sign, the reference cell is placed so that its electrode plates are parallel to the sample cell electrodes, and vice versa.

A sinusoidal voltage at frequency ω was applied to the reference cell to compensate for the retardation created by the sample cell. The null condition was detected at 2ω. High sensitivity (10^{-6} rad) is attained with this technique. The Kerr constant for the unknown sample can be determined by

$$B_{\text{sample}} = B_{\text{ref}} \frac{l_{\text{ref}}}{l_{\text{sample}}} \left(\frac{V_{\text{ref}}/d_{\text{ref}}}{V_{\text{sample}}/d_{\text{sample}}} \right)^2$$

where l_{ref} and l_{sample} are electrode spacings of the two cells. The experimental apparatus for measurement of Kerr constants was similar to that built by Burnham et al.[11] The probe beam was a 10 mW He−Ne red laser (Melles Griot, Model 05LHP 991) with beam diameter 0.68 mm. Red light was chosen since our polyamide samples do not absorb in this region. Plane polarizer sheets were used as polarizers. Note that the value of the Kerr constant is independent of the polarizer efficiency.

The Kerr cell electrodes were stainless steel plates with dimensions 2 cm × 10 cm × 0.8 cm. These were separated by Teflon spacers 3 mm thick. Both the cells were made of Pyrex glass, with circulation jackets to provide isothermal condition at temperature between 5 and 70 °C. We used custom made Teflon O-rings to seal the cells because THF attacks conventional viton O-rings. The detector used was a silicon photodiode (Oriel Corp., Model 7182). The senusoidal signal of 10 V peak at 140 Hz from the signal generator (Wavetek, Model 75) was amplified by an audiopower amplifier to 420 V peak. The power amplifier was built using two power operational amplifiers (APEX μTech, Model PA85) driven by a ±220 V DC power supply (Kikusui Electronics Corp., Model PAB350-0.2). The output of the power amplifier was fed to a 1:10 step up transformer (Gavagan Electronics, Model 8540) to provide 4.2 kV peak across each Kerr cell. The voltages across each cell were varied independently by adjusting the output of the signal generator between 0 and 10 V peak. The phase difference between the voltage signals applied to the two cells was reduced to zero by the phase adjust option of a Tektronix Model 2232 digital oscilloscope. The signal from the detector was fed to a phase sensitive amplifier (Stanford Research Systems, Inc., Model SR510) locked in at 2 times the frequency of the reference signal from the signal generator. High voltages were measured using a 1000:1 probe and a Hewlett Packard Model 3478A digital voltmeter. The reference liquid used was CS_2. The Kerr constant, B_{ref}, of CS_2 at required temperatures was obtained from *International Critical Tables*.[24]

The polyamide samples are sensitive to the moisture level in the solvent (THF) due to aggregate formation by H-bonding. Hence, in order to get true molecularly dispersed solutions, anhydrous 99.9% THF (Aldrich Chemical Co.) was used. Water content was determined to be <0.003% by Karl−Frischer analysis. All solutions were prepared, stored, and transferred to sample cells in a sealed glovebag purged with nitrogen dried over drierite. The glovebag was purged six to seven times after each transfer of material.

Due to the high voltages applied in the Kerr effect experiment, it was found that it was necessary to keep the electrical conductivity of the solvent <0.1 $(M\Omega\ cm)^{-1}$ to avoid electric shorting of the high-voltage circuit. In order to achieve such low electrical conductivity, solvent should be free of ionic impurities. The solvents in which the polyamide sample is soluble are acetone, 1,1,3,3-tetramethylurea (TMU), dimethylacetamide (DMAc), dimethylformamide (DMF), and tetrahydrofuran (THF). The solvent choice was based on their inertness to the insulation and coatings in contact with the solvent. For example, the use of TMU, DMAc, and DMF was avoided because these solvents, unlike THF, attack PVC coatings of insulated wires and enamel coatings of copper wires. We were able to reproduce the literature values of Kerr constants of different solvents within 5%.

Table 1. Characterization Data for the Model Compound (Figure 1b)[a]

melting point (by DSC)	307.15−312.4 °C
infrared (KBr)	3435, 3305, 1660, 1593, 1538, 1492, 1417, 1325, 1250, 1176, 1121, 1076, 1057, 902, 837, 693 cm^{-1}
MS (FAB)	529 (M + 1), 460, 307, 289 *m/e*
^{1}H NMR (DMSO-d_6)	10.7 (s, 2H, N*H*), 8.38 (d, J = 1.85 Hz, 2H), 8.13 (d of d, J = 8.4, 1.8 Hz, 2H), 8.02 (d, J = 6.96 Hz, 4H) 7.61 (m, 6H), 7.4 (d, J = 8.45 Hz, 2H) ppm
^{13}C NMR (DMSO-d_6)	166.04, 139.54, 134.5, 132.32, 131.97, 131.41, 128.52, 127.82, 125.71, 122.48, 122.08, 117.16 ppm

[a] s = single, d = doublet, d of d = doublet of a doublet, m = multiplet.

Wide Angle Light Scattering. The instrument used was a SOFICA light scattering apparatus. The light source was a polarized He−Ne laser, which provides a beam at wavelength 633 nm. The sample cell was a 1 in. diameter Pyrex glass vial containing the polymer solution. The sample cell was sealed using Teflon tape inside a drybag to prevent moisture from contaminating the polymer solution.

Depolarized Light Scattering. The instrument used was a light-scattering apparatus with a Spectra Physics 165 Ar ion laser source, which provided a beam with wavelengths of 515 and 488 nm. Relative intensity measurements were done for pure solvent and solutions using 10 mm diameter Pyrex glass test tubes. Intensity readings were recorded for 10 different positions of the test tube for both H_v and V_v configurations. The depolarization ratio was obtained after subtracting the scattering due to solvent from the H_v and V_V scattering from the solution.

Differential refractive index increments (dn/dc) at 633 nm were measured with a Chromatix (LDC Milton Ray) KMX-16 differential refractometer. The KMX-16 instrument was calibrated with aqueous sodium chloride solutions (dn/dc = 0.174 at 633 nm at 25 °C).

Model Compound Synthesis. 2,2′-Bis(trifluoromethyl)-benzidine (Marshallton Laboratory) (3.6960 g, 11.5 mmol) and benzoyl chloride (3.2456 g, 23.1 mmol) were stirred together in dry pyridine (50 mL) at room temperature overnight). The colorless solid that precipitated out was filtered, washed with distilled water on the frit, and dried. Purification of dried solid product was attempted by crystallization from ethanol. Upon cooling, 0.2934 g of powdery solid (A) precipitated which was filtered and dried under vacuum. Mother liquor was concentrated to give additional 2.044 g of solid (B) which was dried. A and B were combined because these solids were characterized to be the desired product by melting point, infrared absorption peaks, mass spectrometry, and chemical shifts of proton and ^{13}C NMR. This analytical data is listed in Table 1. CF_3 is not detected due to broadening because of C−F coupling.

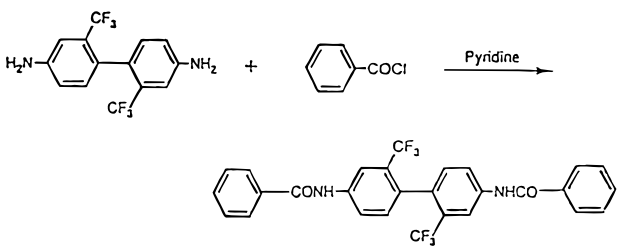

Results and Discussion

Kerr Effect. Three samples labeled M1, M2, and M3 with different molecular weights were used for this study. Their exact molecular weights will be ascertained by combining the Kerr effect data and the wide angle light-scattering data.

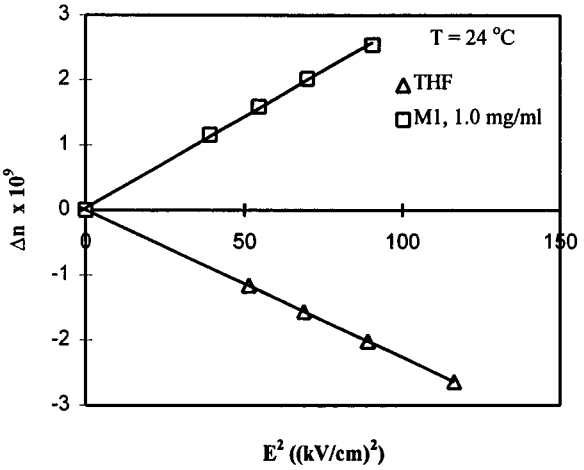

Figure 2. Kerr law for THF and M1 in THF (1.0 mg/mL) at 24 °C.

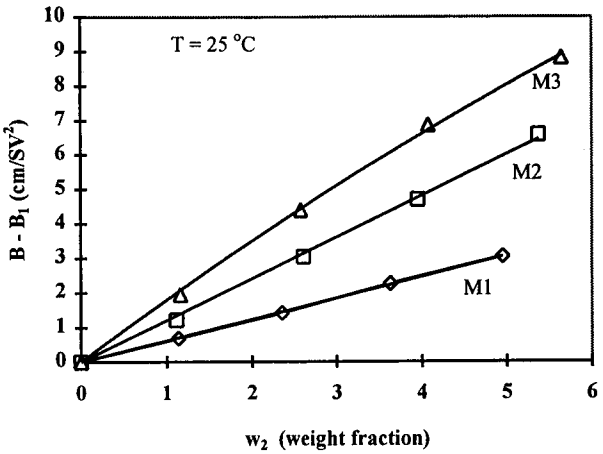

Figure 3. Excess Kerr constant for samples M1−M3 in THF at 25 °C as a function of polymer weight fraction.

The electric birefringence experiment was performed on four solutions of each sample, with increasing concentration in THF. For each solution, null technique was used to balance the retardation over a range of electric field from about 5 to 10 kV/cm. A linear dependence was found in accordance with the Kerr law in each case. Figure 2 shows Δn plotted against square of the electric field for pure solvent (THF) and for a 1.0 mg/mL solution. The Kerr law is obeyed in both cases shown. The induced electric birefringence of THF is negative and becomes positive upon addition of polyamide to the solvent. This implies that the net birefringence will be zero at some concentration between 0 and 1.0 mg/mL. Hence it is desirable to perform the experiment over a concentration range before drawing conclusions about the Kerr effect of a given polymer sample. It is clear that the Kerr effect of polyamide must be positive since it increases the Δn of the solution. The Kerr constant of THF is negative because its axis of maximum polarizability is perpendicular to its permanent dipole moment. The slope of the lines in Figure 2 is the Kerr constant (B) of the solution and B_1 of the solvent. The excess Kerr constant, $B - B_1$, is plotted as a function of polyamide weight fraction, w_2, in Figure 3 for samples M1−M3. From these curves we conclude that molecular weight of M3, M2, and M1 should decrease in that order. The slope of each line is the constant a_4 required in eq 2 to calculate the specific Kerr constant at infinite dilution ${}_sK_2$.

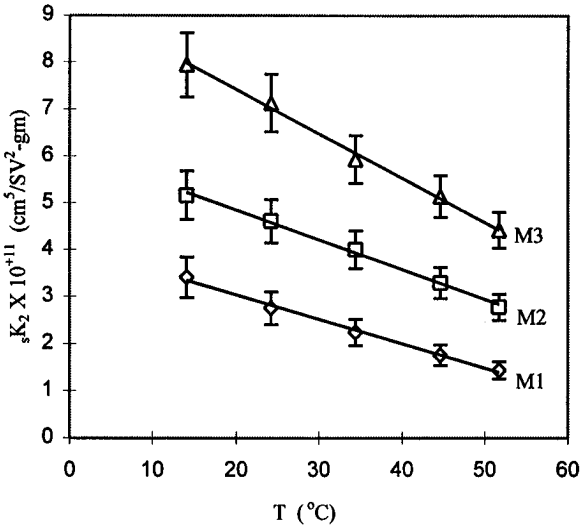

Figure 4. Temperature dependence of the specific Kerr constant, ${}_sK^2$, for samples M1−M3.

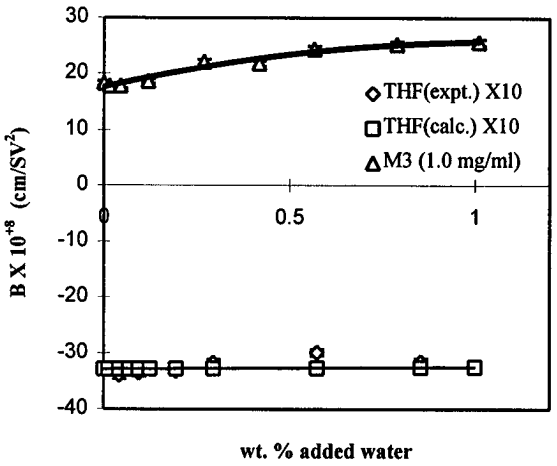

Figure 5. Kerr constants as a function of weight percent added water, for THF and M3 in THF at 24 °C.

For our system it was found that a_1, a_2, and a_3 are negligible compared to a_4. This experimental value of ${}_sK_2$ gives an average value of $[(\alpha_{||} - \alpha_{\perp})^2/M]_{ave}$ due to polydispersity of the samples according to eq 3. Equation 4 is used in the next section along with the two WALS equations to calculate the unknowns—persistance length (a), weight average degree of polymerization (n_w), and optical unit anisotropy ratio (ϵ).

The effect of temperature on the Kerr constant of the polyamide solution is studied by cooling and heating the solution. Figure 4 shows the variation of specific Kerr constant ${}_sK_2$) for samples M1−M3 over a temperature range from 10 to 50 °C. As the temperature increases, ${}_sK_2$ decreases approximately linearly. Since ${}_sK_2$ is directly proportional to $(\alpha_{||} - \alpha_{\perp})^2$, optical anisotropy of the chain decreases with temperature. The rotation of adjacent groups with increasing temperature makes the chain more coil-like or flexible, causing a decrease in its optical anisotropy.

To evaluate the effect of moisture on the Kerr constant, we performed electric birefringence experiments on samples contaminated with known amounts of water. Results of these experiments are shown in Figure 5. The lower line is for Kerr constant of pure THF with different quantities of water added to it. The theoretically calculated Kerr constant of these solutions, assuming additivity of specific Kerr constants of water

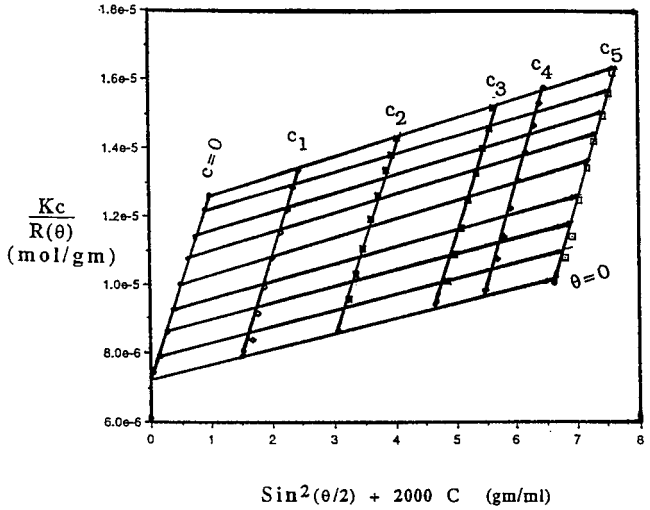

Figure 6. Zimm plot of elastic light scattering from solutions of sample M2 in THF at 25 °C obtained with the SOFICA light-scattering instrument. Concentrations in mg/mL: $C_1 = 0.765$, $C_2 = 1.557$, $C_3 = 2.360$, $C_4 = 2.778$, and $C_5 = 3.343$.

and THF based on weight fractions, is also shown. The experimental values agree very well with the calculated values. This serves to illustrate two points. Firstly, it indicates that the experimental error is much less than the change in B caused by the polymer (upper curve). Secondly, the increase in Kerr constant seen in the upper curve for M3 solution is actually due to changes in the polyamide structure rather than to excess water itself since the lower curve for water in THF is fairly flat. There is no change in the Kerr constant within experimental error until about 0.1% added H_2O. Above this concentration of water, there is a distinct increase in the Kerr constant. This may be due to aggregation of polyamide molecules by H-bonding with water, that is, water molecules may form a bridge between two polyamide molecules which could cause the formation of aggregates of chains arranged somewhat parallel to each other. Moreover, the Kerr constant could increase further due to increase in stiffness of the polyamide upon formation of such aggregates. The Kerr constant can also increase due to water molecules preferentially aligning along the polymer backbone and hence increasing the inherent anisotropy ratio of the optical unit. These experiments clearly indicate that it is critical to keep the solution free of moisture in order to obtain a true molecular dispersion. Next we measured the apparent molecular weight and radius of gyration by WALS to determine the molecular parameters of the polymer chain.

Wide Angle Light Scattering. The data for sample M2 is plotted in the form of conventional Zimm plot of $Kc/R(\theta)$ versus $\sin^2(\theta/2) + 2000c$ as shown in Figure 6. The molecular weight and radius of gyration obtained from these plots are apparent quantities due to the anisotropic nature of the scattering segments. The parameters M_{app}, R_{gapp}, and A_{2app} were determined by extrapolation of $Kc/R(\theta)$ to $c = 0$ and $\theta = 0$.

The modified light-scattering theory developed by Nagai[17] for a persistent wormlike polymer chain, to incorporate polydispersity effect, that relates M_{app} and R_{gapp} to molecular parameters has been discussed earlier. Equations 6a and 6b from WALS and eq 4 from electric birefringence experiment have been solved numerically for the unknown molecular parameters a, ϵ, and n_w. The degree of polymerization (n_w), persistence length (a), and optical unit anisotropy ratio (ϵ) calculated from WALS and Kerr effect measurements are listed in Table 2.

Table 2. Molecular Parameters of Polyamide

sample	n_w	a (Å)	ϵ
M1	170 ± 18	210 ± 50	2.0 ± 0.3
M2	390 ± 40	210 ± 40	2.5 ± 0.3
M3	390 ± 40	230 ± 50	2.6 ± 0.4
sample	M_w	R_{gz}	$\sqrt{R^2}/L$
M1	55 000 ± 6000	400 ± 50	0.5
M2	130 000 ± 14 000	600 ± 60	0.3
M3	130 000 ± 13 000	660 ± 50	0.3

The persistence length and the optical unit anisotropy ratio are independent of molecular weight within the experimental error indicating that wormlike chain model can successfully represent the real chain. The molecular weights and radii of gyration are also given in Table 2. Samples M2 and M3 have approximately equal molecular weights within the experimental error. Although considering the error bars in Figure 4 for the specific Kerr constant values, the molecular weight of M3 is likely to be slightly larger than that of M2. Fractional chain extension is the ratio of the root-mean-square end-to-end distance to the contour length of the chain. This ratio is unity for a rigid rod and equal to $1/\sqrt{n_k}$ for a Gaussian coil with n_k Kuhn statistical segments. For all three samples, this ratio is approaching unity indicating the semiflexible nature of these polyamides.

As discussed earlier, there is evidence indicating that aggregates of polyamide are formed on addition of water. This is expected since a H_2O molecule can form a bridge between two amide groups by H-bonding. We feel confident that no aggregates of 2,2′-disubstituted biphenyl polyamides are formed in THF provided the system is kept moisture free ($H_2O < 0.005\%$) because the molecular parameters obtained above are in fairly good agreement with those obtained from dilute solution viscometry and depolarized light-scattering experiments, which were conducted under similar moisture free conditions. This is surprising since THF has a low dielectric constant and hence should not reduce the attractive electrostatic forces between the H and O atoms of the two amide groups forming a H-bond. Moreover, this behavior is unlike single phenyl polyamides like Kevlar which form H-bonds very easily. Since these hydrogen bonds cannot be broken by low dielectric constant solvents like THF, they are soluble only in strong acids.

The explanation of this observation lies in the chemical structure of the polyamide we are studying. In 2,2′-disubstituted biphenyl polyamides, hydrogen bonding is expected to be weakened as a result of noncoplanar phenyl rings and increase in the hydrogen bond distance to 7 Å.[4−6]

Differential Refractometry. The dn/dc values for M1−M3 in THF are within experimental error, and the mean value is 0.133 ± 0.004 mL/g. The dn/dc values for polyamide M1 measured in TMU and that for the model compound in THF are 0.112 ± 0.004 and 0.151 ± 0.004 mL/g, respectively. Using the dn/dc values for M1 in THF and TMU in the Dale−Gladstone relation, we get $n_2 = 1.67 \pm 0.03$ and density = 2.00 ± 0.12 g/mL. Obtained density is comparable to other fluorinated polymers, such as poly(tetrafluoroethylene), with a density of 2.280−2.290 g/mL for the polymerized sample and 2.302 g/mL for the crystalline sample.[25] Assuming that the specific volume of the model compound is the

Table 3. Optical Parameters of Polyamide Samples M1−M3 and the Model Compound

sample	n_2	$\alpha_o \times 10^{23}$ (cm^3)	ϵ	$(\alpha_1 - \alpha_2) \times 10^{23}$ (cm^3)
polyamide[a]	1.67 ± 0.03	2.45 ± 0.20	2.4 ± 0.3	5.9 ± 1.3
model compound	1.71 ± 0.03	2.55 ± 0.19	1.5 ± 0.2	3.8 ± 0.8
bond additivity[b]		2.96		1.0

[a] Mean value. [b] Reference 4.

same as that of the polyamide, the refractive index of the model compound calculates to be 1.71 ± 0.03.

The mean optical polarizability of the optical unit is calculated from the refractive indices using the Lorentz−Lorenz equation. The results of these calculations are listed in Table 3. The mean polarizabilities of the polymer are in good agreement with those of the model compound. The optical unit anisotropy ratio of the model compound, ϵ, is calculated from the measured depolarization ratio of 0.120 ± 0.024 at 515 nm, using the relation $\rho_v = \epsilon^2/(15 + (4\epsilon^2/3))$. This equation is valid strictly for small molecules. We have assumed the wavelength dependence of optical polarizabilities to be negligible between 633 and 515 nm, since these wavelengths are far removed from the absorption region of the model compound (UV region). The optical unit anisotropy was calculated using $\alpha_1 - \alpha_2 = \epsilon\alpha_o$.

The refractive index and mean polarizability for the polyamide and the model compound are in excellent agreement, while the optical unit anisotropy ratio (ϵ) and optical unit anisotropy ($\alpha_1 - \alpha_2$) are not in agreement. This may be due to the model compound forming aggregates in solution. The mean polarizability is independent of aggregation, while anisotropy of polarizability is very sensitive to aggregate formation. Note that steric hindrance cannot prevent aggregation since the amide group of the model compound can be approached from various directions by that of another molecule. The mean polarizability and anisotropy of the optical unit calculated from bond additivity[4] are not in agreement with the experimental data. This is expected since the bond additivity does not hold for molecules having extended conjugation.

Nonlyotropic Behavior. This polyamide does not exhibit liquid crystalline behavior in either solid state or solution. The axial ratio of the polymer is 12.5 based on a persistence length of 200 Å and a chain diameter of 16 Å which was estimated by molecular modeling.[26] In order to understand this behavior in more detail, we have applied the treatment of Flory,[27] Onsager,[28] Ishihara,[29] and Odijk.[30] The latter deals specifically with semiflexible chains, and the minimum volume fraction of polymer, v_2, for formation of a stable anisotropic phase according to this theory is given by $v_2 = k_c/z$, where z is the axial ratio of the rod and k_c is a function of L/a). For the polyamide studied, $k_c \sim 5.6$, leading to a critical volume fraction of 0.45. Our polymer precipitates at a volume fraction of 0.13, and Flory's and Ishihara's equations give critical volume fractions of 0.54 and 0.27, respectively. Hence it may be concluded that even though these polymers are soluble in a variety of common solvents to quite high concentrations which significantly exceed that of poly(*p*-phenyleneterethalamide) and its homologues, and they have persistence lengths in the same range as the latter, they do not form lyotropic solutions because the solubility limit is much lower than the critical concentration. Furthermore, this polymer does not exhibit liquid crystalline behavior in the solid state even though it has an axial ratio of 12.5, which is 2 times as large as that predicted by Flory. Steric hindrance to close packing due to CF_3 groups may play an important role. Factors such as specific interactions and efficiency of packing have not been considered in the theories of Flory, Onsager, Ishihara, and Odijk.

Conclusions

We conclude that the high persistence length of the polymer molecule (220 ± 50 Å) and the high optical anisotropy of the optical unit (2.2 ± 0.3) result in the very high birefringence ($\Delta n = 0.7$) observed for the oriented films of these polyamides. Furthermore, the rodlike shape of the chain makes it more amenable to orientation upon stretching.

The aromatic polyamide studied is satisfactorily modeled as a Kratky−Porod wormlike chain. Excluded volume effect seems to be negligible in THF at 25 °C, since the Kratky−Porod model does not include excluded volume interactions. It is also conclusively established that no aggregates are formed in THF free of moisture.

Refractive index of 1.67 ± 0.03 obtained from differential refractometry is in good agreement with that of 1.67−1.76 for similar polyamides.[4] The mean polarizability and anisotropy of the optical unit calculated from bond additivity[4] are not in agreement with the experimental data, since the bond additivity approximation does not hold for molecules having extended conjugation.

The polyamide does not exhibit lyotropism inspite of its high persistence length comparable to Kevlar because its solubility limit is much lower than its critical concentration for formation of a stable anisotropic phase. Furthermore, Flory's theory is unable to explain the nonliquid crystalline behavior in the solid state. Factors such as steric hindrance to efficient packing due to bulky side groups and specific interactions, which are not considered in Flory's theory, may play an important role in determining the lyotropic behavior.

Acknowledgment. We gratefully acknowledge partial financial support from the National Science Foundation. We also thank Mr. Anthony Castellano (IBM Watson Research Center) for his help in designing and building the Kerr effect apparatus, Prof. David Hoagland and Prof. Kenneth Langley for their laboratory support regarding light scattering, and Prof. Scott Barton for his valuable suggestions.

Appendix

The functions A and B are appearing in the light-scattering eq 11 are as follows:

$$A = \frac{2}{y} + \frac{14\epsilon^2}{135}(\mathrm{G2})$$

$$B = \frac{4a^2\epsilon}{135}(\mathrm{G3}) - \frac{a^2}{9}(\mathrm{G1}) - \frac{11a^2\epsilon^2}{5670}(\mathrm{G4})$$

where

$$\mathrm{G1} = \frac{6\beta}{y^2} - \frac{6}{y} + \frac{6}{\beta} - \frac{6y}{\beta^2} + \frac{6y^2}{\beta^2(y+\beta)}$$

$$\mathrm{G2} = \frac{1}{\beta} - \frac{y}{3\beta^2} + \frac{y^2}{3\beta^2(y+3\beta)}$$

$$G3 = \frac{2}{y} - \frac{4(42+\epsilon)}{63\beta} + \frac{(1638+51\epsilon)y}{567\beta^2} - \frac{(30+\epsilon)y^2}{10\beta^2(y+\beta)} + \frac{(42+5\epsilon)y^2}{378\beta^2(y+3\beta)} - \frac{\epsilon y^2}{63\beta(y+3\beta)^2} + \frac{\epsilon y^2}{315\beta^2(y+6\beta)}$$

$$G4 = \frac{1}{\beta} - \frac{97y}{66\beta^2} - \frac{189y^2}{110\beta^2(y+\beta)} - \frac{19y^2}{66\beta^2(y+3\beta)} + \frac{y^2}{11\beta(y+3\beta)^2} + \frac{13y^2}{330\beta^2(y+6\beta)}$$

References and Notes

(1) Kwolok, S. L. U.S. Patent 3 671 542, 1972.
(2) Morgan, P. U.S. Patent 3 801 528, 1974.
(3) Blades, H. U.S. Patent 3 869 429, 1975.
(4) Rogers, H. G.; Gaudiana, R. A.; Hollinsed, W. C.; Kalyanaraman, P. S.; Manello, J. S.; McGowan, C.; Minns, R. A.; Sahatjian, R. *Macromolecules* **1985**, *18*, 1058.
(5) Gaudiana, R. A.; Sinta, R. F. *J. Polym. Sci., Part A: Polym. Chem.* **1991**, *29*, 45.
(6) Stein, R. S.; Sethumadhavan, M.; Gaudiana, R. A.; Adams, T.; Guarrera, D.; Roy, S. K. *J. Macromol. Sci.-Pure Appl. Chem.* **1992**, *A29* (7), 517.
(7) Gaudiana, R. A.; Minns, R. A.; Sinta, R.; Weeks, N.; Rogers, H. G. *Prog. Polym. Sci.* **1989**, *14*, 47.
(8) Khanarian, G.; Tonelli, A. E. *J. Chem. Phys.* **1981**, *75*, 5031.
(9) Lefevre, C. G.; LeFevre, R. J. W. In *Techniques of Chemistry*; Weissberger, A., Ed.; Wiley-Interscience: New York, 1972; Vol. I, Part IIIc, Chapter VI.
(10) Flory, P. J.; Saiz, E. *J. Phys. Chem.* **1981**, *85*, 3215.
(11) Burnham, A. K.; Buxton, L. W.; Flygare, W. H. *J. Chem. Phys.* **1977**, *67*, 4990.
(12) Lezov, A V.; Tsvetkov, N. V.; Trusov, A. A. *Polym. Sci. U.S.S.R.* **1990**, *32*, 1801.
(13) Tsvetkov, V. N. In *Rigid Chain Polymers*; translated by Korolyova, E. A.; Consultants Bureau: New York, 1989; Chapter VII.
(14) Ebert, M.; Jungbauer, D. A.; Kleppinger, R.; Wendorff, J. H. *Liq. Cryst.* **1989**, *4*, 53.
(15) Jungbauer, D. A.; Wendorff, J. H. *Mackromol. Chem.* **1988**, *189*, 1345.
(16) Yamakawa, H. *Modern Theory of Polymer Solutions*; Harper and Row: New York, 1971; Chapter II.
(17) Nagai, K. *Polym. J.* **1972**, *3*, 67.
(18) Kerr, J. *Philos. Mag.* **1875**, *50* (4), 337, 446.
(19) Le Fevre, C. G.; Le Fevre, R. J. W. *J. Chem. Soc.* **1953**, 4041.
(20) Buckingham, A. D.; Pople, J. A. *Proc. Phys. Soc. London* **1955**, *A68*, 905.
(21) Flory, P. J. *Chem. Rev.* **1946**, *39*, 137.
(22) Flory, P. J. In *High Molecular Weight Organic Compounds (Frontiers in Chemistry)*; Burk, R. E., Grummitt, O., Eds.; Interscience: New York, 1949; Vol 6.
(23) Zimm, B. H. *J. Chem. Phys.* **1948**, *16*, 157.
(24) *International Critical Tables, VII*; McGraw Hill: New York, 1930.
(25) Brandrup, J., Immergut, E. H., Eds. *Polymer handbook*; John Wiley and Sons: New York, 1975.
(26) (a) Irwin, R. S.; Vorpagel, E. R. *Macromolecules* **1993**, *26*, 3391. (b) Private communication.
(27) Flory, P. J. *Proc. Roy. Soc. London, Ser. A* **1956**, *234*, 73.
(28) Onsager, L. *Ann. N. Y. Acad. Sci.* **1949**, *51*, 627.
(29) Ishihara, A. *J. Chem. Phys.* **1950**, *18*, 1446; **1951**, *19*, 1142.
(30) Odijk, T. *Macromolecules* **1986**, *19*, 2313.

MA951777T